American Mineralogist, Volume 91, pages 29–34, 2006

The real topological configuration of the extra-framework content in alkali-poor beryl: A multi-methodological study

G. DIEGO GATTA,[1,2,*] F. NESTOLA,[2] G.D. BROMILEY,[2,3] AND S. MATTAUCH[4]

[1]Dipartimento di Scienze della Terra, Universita' degli Studi di Milano, Via Botticelli 23, I-20133 Milano, Italy
[2]Bayerisches Geoinstitut, Universitaet Bayreuth, Universitaet Str. 30, D-95447 Bayreuth, Germany
[3]Department of Earth Sciences, Cambridge University, Downing Street, Cambridge CB2 3EQ, U.K.
[4]Forschungszentrum Jülich, D-52425 Jülich, Germany

ABSTRACT

The crystal structure of alkali/water-poor beryl ($H_2O + Na_2O + Cs_2O < 1.2$ wt%) was reinvestigated by means of laser ablation inductively coupled plasma mass spectroscopy, thermogravimetric analysis, neutron diffraction, and polarized infrared spectroscopy to determine the real topological configuration of the extra-framework content in the six-membered ring channels. Analysis of the nuclear density Fourier map suggests that the (water) oxygen is located along the sixfold axis at the 2*a* site (0,0,1/4), whereas the (water) protons are at –0.028(7), –0.071(3), 0.332(1). The hydrogen atoms are distributed in 6×2 equivalent positions, above and below the oxygen site. Geometrical configuration of the water molecule is well defined: the O-H bond distance is 0.949(18) Å and the H-O-H bond angle is 106.9(2.2)°. The H···H vector is oriented at ~4° from [001]. This configuration is completely different from that found in alkali-rich beryl, where the H···H vector is perpendicular to [001]. Na is probably located, with the H_2O oxygen, at the 2*a* site. According to the chemical analysis, which shows that the amounts of other alkali and earth-alkali cations are negligible (Rb, K, Mg, Mn ≤ 110 ppm, Ca ≤ 225 ppm, Cs ≤ 430 ppm), no effect of other cations on the extra-framework population was observed in the structural refinement. The final agreement index (R_1) of the structural refinement was 0.037 for 34 refined parameters and 160 unique reflections with $F_o > 4\sigma(F_o)$. The topological configuration of the H_2O molecule into the channel is confirmed by the spectroscopic investigation. Polarized single-crystal IR spectra show that the H_2O molecule is oriented with the molecular symmetry axis perpendicular to the hexagonal axis and H···H vector parallel (or quasi-parallel) to [001].

Keywords: Chemical mineral analysis, L-A-ICP-MAS, crystal structure, single-crystal neutron diffraction, water-poor beryl, polarized IR-spectra, trace elements, REE

INTRODUCTION

Several experimental and theoretical studies have been carried out on the crystal-chemistry, high-temperature, and high-pressure behavior of natural and synthetic beryl with different extra-framework contents (Bragg and West 1926; Wood and Nassau 1967, 1968; Gibbs et al. 1968; Goldman et al. 1978; Morosin 1972; De Almeida et al. 1973; Hawthorne and Černý 1977; Aines and Rossman 1984; Brown and Mills 1986; Hazen et al. 1986; Aurisicchio et al. 1988; Schmetzer 1989; Sheriff et al. 1991; Artioli et al. 1993; Charoy et al. 1996; Kolesov and Geiger 2000a; Prencipe 2002). Beryl is an accessory mineral found mainly in pegmatitic rocks, with the ideal chemical formula $Al_2Be_3Si_6O_{18}$ (space group *P*6/*mcc*). The crystal structure consists of six-membered rings of SiO_4 tetrahedra, perpendicular to the [001] axis, linked by AlO_6 octahedra and BeO_4 tetrahedra to form a three-dimensional framework (Fig. 1). Alkali cations (Cs, Rb, K, Na) and water molecules represent the so-called "extra-framework content", which lies within the six-membered ring channels along [001]. The presence of such cations is due to a charge imbalance in the framework because of the isomorphic substitution of Al and Be by lower valency cations ($Al^{3+} \leftrightarrow Mg^{2+}$, $Fe^{2+/3+}$, Mn^{2+}, Cr^{3+}, V^{3+}, and $Be^{2+} \leftrightarrow Li^{+}$), yielding the representative chemical formula $(Cs,Rb,K,Na)_{x+y}Al_{2-x}Me^{2+}_{x}Be_{3-y}Li_ySi_6O_{18}\cdot zH_2O$ ($0 < x + y < 1$). Despite the large number of studies devoted to the crystal chemistry of beryl, the exact topological configuration of the extra-framework content remains uncertain, especially for alkali-poor samples. On the basis of X-ray single-crystal diffraction data, several studies (Gibbs et al. 1968; Hawthorne and Černý 1977; Brown and Mills 1986; Aurisicchio et al. 1988; Ferraris et al. 1998) have shown that the extra-framework population is located at two distinct sites along the sixfold symmetry axis: 0,0,0.25 (Wyckoff 2*a* position) and 0,0,0 (2*b*). Aurisicchio et al. (1988) suggested that water molecules are present at the 2*b* site, and that the extra-framework cations are located at the 2*a* site. In contrast, other authors (Gibbs et al. 1968; Hawthorne and Černý 1977; Brown and Mills 1986; Ferraris et al. 1998) reported water molecules and large cations (Cs, Rb, K) at the 2*a* site, with smaller cations (such as Na) at the 2*b* site. A single-crystal neutron diffraction study of an alkali/water-rich beryl and an alkali/water-poor beryl performed by Artioli et al. (1993) showed two distinct topological configurations of the extra-framework

* E-mail: diego.gatta@unimi.it

content on the basis of the alkali/water amount. In beryl with a high content of water and cations (H_2O 1.70 wt%, $Na_2O + Cs_2O$ 3.19 wt%), the oxygen atoms of H_2O molecules were located at the 2*a* site and the H···H vectors lay on a plane parallel to (001), and the Cs and Na cations partially occupied the 2*a* and the 2*b* sites, respectively. The environment of the water molecule was well defined: bond-distances and angles showed reasonable values. The orientation of the H···H vector, parallel to the (001) plane, also confirmed the spectroscopic evidence of Wood and Nassau (1967, 1968) and Aines and Rossman (1984) for alkali/water-rich beryls. However, Artioli et al. (1993) were not able to give a unique explanation for the topological configuration of the channel content in alkali-poor beryl (H_2O 0.90 wt%, $Na_2O + Cs_2O$ 0.09 wt%). In fact, in this case the location of H_2O oxygen (and Na) at the 2*a* site and the H at 0,0,0.16(1), based on the difference-Fourier map, gave rise to a physically non-acceptable geometrical configuration of the water molecule, with an H-O-H angle of 180º and an O-H bond distance of ~0.78 Å. The authors provided some possible explanations, based on possible static disorder of one of the protons or of the oxygen atom, but the problem was basically unsolved. Some recent experimental and theoretical studies, based on spectroscopic investigations and ab initio charge density analysis (Kolesov and Geiger 2000a; Prencipe 2002), gave some new insights into the crystal chemistry of alkali-free (or alkali-poor) beryl. However, no experimentally obtained structural data are, at present, available to define unambiguously the configuration of the extra-framework population in alkali-poor beryl.

The aim of this work is to reinvestigate of the crystal structure and crystal chemistry of a natural alkali-poor beryl by means of laser ablation inductively coupled plasma mass spectroscopy, thermogravimetric analysis, single-crystal neutron diffraction, and polarized infrared spectroscopy to define the real topological configuration and location of water molecules and cations that lie within the six-membered ring channels. Current neutron facilities and improvements in other techniques can now provide us with more accurate and precise data, allowing us to reinvestigate the crystal chemistry of materials with very low amounts of "zeolitic water".

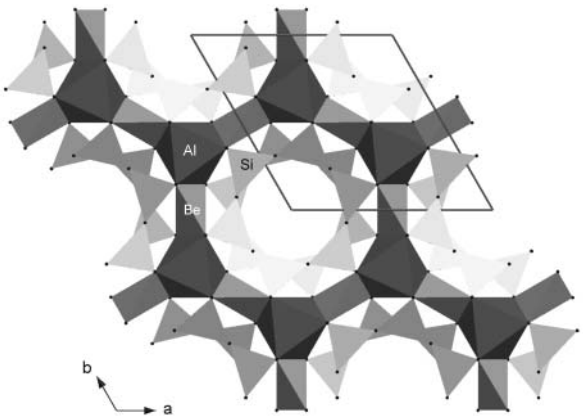

FIGURE 1. The crystal structure of beryl viewed down [001].

EXPERIMENTAL METHODS

A natural, colorless, and transparent, gem-quality single-crystal of a pegmatitic beryl (~2.5 cm^3) from Shengus, Haramosh Mountains, Gilgit, Northern Areas, Pakistan, kindly provided by the Italian collector S. Ancona, was used in this study. In polarized light the crystal appeared free of defects, inclusions, or zoning. The sample was cut into four parts, to perform the chemical and thermogravimetric analysis, neutron diffraction experiment, and IR investigation.

One of the single crystals was studied by means of electron microscopy at the Bayerisches Geoinstitut (BGI) using a Leo Gemini 1530 scanning electronic microscope with field emission electron gun. The crystal appeared free of defects and zoning, confirming the previous optical observations, and the qualitative (semi-quantitative) analysis carried out with the energy dispersive system showed a low amount of Na and Fe (close to the detection limit) and the absence of Cs, Cr, V, or other high-*Z* elements. The amount of SiO_2 was then carefully measured with a fully automated CAMECA SX-50 microprobe using the wavelength dispersive system (WDS) at the BGI (operating conditions: 15 kV, beam current of 20 nA, albite used for Si*K*α lines as reference standard) to be used for the further chemical investigation (see below). The same crystal was then used for chemical analysis by means of laser ablation inductively coupled plasma mass spectroscopy (LA-ICP-MS) at the Earth Science Department, University of Perugia, Italy, with a laser ablation system made by NeW Wave UP213 (Nd:YAG laser source) coupled with a Thermo Electron X7 ICP-MS. The system was optimized for dry plasma conditions and a continuous ablation of NIST SRM 612 by maximimizing the signals from selected masses (La^+ and Th^+) and reducing oxide formation measured by ThO^+/Th^+. Calibration was performed using NIST SRM 612 as an external calibration sample in conjunction with internal standardization using Si, previously measured by EMPA-WDS (Longerich et al. 1996). Optimum data acquisition parameters (quadrupole settling time, dwell time, points per spectral peak) and data reduction algorithms followed the Longerich et al. (1996) protocol. The following masses (isotopes) were analyzed: ^{7}Li, ^{9}Be, ^{23}Na, ^{24}Mg, ^{27}Al, ^{29}Si, ^{39}K, ^{44}Ca, ^{55}Mn, ^{56}Fe, ^{85}Rb, and ^{133}Cs. The chemical composition of sample is reported in Table 1.

A second crystal was used for the thermal analysis performed at the Department of Chemistry, University of Perugia, with a NETZSCH STA 449C instrument using 7.442 mg of powdered sample, previously dried at 130 ºC for 4 h. The sample was ground (final crystallite size 10–15 μm) using a tungsten carbide mortar, instead of an agate mortar, to avoid any contamination of the sample due to the hardness of beryl. The thermal curve (weight loss vs. *T*, obtained in air and by increasing the temperature by 1 ºC/min), showed a monotonic trend that became flat at about 1100 ºC. The experiment was conducted up to 1200 ºC. The calculated amount of H_2O, on the basis of the weight loss, is 0.86 wt%.

A third crystal of the beryl sample was used for the spectroscopic investigation. Polarized IR spectra were obtained with a Bruker IFS-120-HR high-resolution spectrometer coupled with a Bruker IR microscope at the BGI. The spectrometer contains a permanently aligned Michelson type interferometer with a 30º angle of incidence to the beam-splitter. A W-light source, an Si-coated CaF_2 beam-splitter, and a narrow-band MCT detector were used for the measurements. The incident radiation was polarized using a wire-strip polarizer on a KRS-5 substrate. To avoid absorption bands due to external contaminants (H_2O vapor or CO_2), the optics of the spectrometer were kept under vacuum and the optics of the microscope were continuously purged with purified air (free of H_2O and CO_2) during the measurements. A variable aperture in the rear focal plane of the 15× microscope objective was used to obtain spectra from a 200 μm area. The resolution of the spectra was 1 cm^{-1}. Infrared spectra were obtained using radiation polarized parallel to **a** and **c** of the beryl samples. To do this, two small single crystals were oriented using a Huber four-circle X-ray diffractometer, and then cut and polished in thin platelets (50 μm

TABLE 1. Chemical composition of the beryl sample

	Oxide wt%	Atoms pfu		wt ppm
SiO_2	66.38	5.93	^{7}Li	182(1)
Al_2O_3	18.29	1.93	^{24}Mg	90(18)
Fe_2O_3	0.42	0.03	^{39}K	109(7)
Na_2O	0.18	0.03	^{44}Ca	225(24)
BeO	13.70	2.94	^{55}Mn	56(2)
H_2O	0.86	0.26	^{85}Rb	32(1)
Total (1)	99.83	(Σ metal ions = 10.86)	^{133}Cs	430(7)
			Tot.(2)	0.112 wt%

$Al_{1.93}Fe_{0.03}Be_{2.94}Si_{5.93}O_{18}\cdot(Na_{0.03}\cdot 0.26H_2O)$

Notes: Major and minor elements were determined by LA-ICP-MS, except for SiO_2 wt% (determined by WDS-EMPA and used as internal standard for the LA-ICP-MS, see text). Given the small amount of Na present, Fe is considered be in the trivalent state.

thick) with the polished surfaces parallel to (001) and (100) respectively.

A fourth crystal from the beryl sample was used for the neutron diffraction experiment. A preliminary test of the crystal ($1.1 \times 1.3 \times 2.0$ mm^3) was performed by means of X-ray diffraction at the BGI using a Huber four-circle diffractometer equipped with non-monochromatized Mo$K\alpha$ radiation. Accurate cell parameters were measured using eight-position centering of 44 Bragg reflections ($5° < 2\theta < 40°$), according to King and Finger (1979) and Angel et al. (2000), giving a metrically hexagonal cell with: $a = b = 9.21168(12)$ Å, $c = 9.19209(22)$ Å, $V = 675.49(2)$ Å^3, $c/a = 0.9978$. According to the Aurisicchio et al. (1988) definition, based on the relationship between c/a ratio and chemical composition, our sample belongs to the "normal beryl group". The single-crystal neutron diffraction experiment was performed at room temperature with a Huber four-circle diffractometer (SV28 beam-line) installed at the DIDO reactor, Forschungszentrum Juelich, Germany. The incident radiation (CW with $\lambda = 1.24126$ Å) was obtained using a Cu(200) monochromator. The neutron flux density was about 2.5×10^6 n·s^{-1}·cm^{-2} and the tangential beam tube led to a very small background count rate (~5 s^{-1}). The unit-cell parameters of the neutron measurement are: $a = b = 9.2099(35)$ Å, $c = 9.1894(18)$ Å ($c/a = 0.9977$). A total of 1534 reflections were recorded with $-8 \le h \le 9$, $-9 \le k \le 8$, and $-9 \le l \le 9$ (maximum $2\theta = 100.78°$), of which 191 were unique. Two standard reflections were measured with a frequency of 450 min throughout the experiment and the intensity variation was within $\sigma(I)$. Further details of the data collection are reported in Table 2. The systematic extinction rules agreed with space group *P6/mcc*. Diffraction data were then corrected for the Lorentz effect. No absorption correction was applied because of the composition and the dimensions of the sample. After correction, the discrepancy factor for the symmetry related reflections was $R_{int} = 0.074$. The high R_{int} value can be reasonably explained by the extinction effects due to the "perfect" crystal sample used in this experiment, as checked by ψ-scan of several Bragg reflections.

Results

Structural refinement

A structural refinement, on the basis of neutron diffraction data, was first carried out with isotropic displacement parameters in space group *P6/mcc* using the SHELXL-97 package (Sheldrick 1997), starting from the atomic coordinates of Artioli et al. (1993) and only considering the framework atoms (i.e., the channels were considered to be completely empty). The scattering lengths of the atoms from the *International Tables for Crystallography C* (Wilson and Price 1999) were used. Due to the negligible amount of Li and Fe, which can substitute for Be and Al respectively, only the scattering length of Be for the tetrahedral site (at 1/2, 0, 1/4) and of Al for the octahedral site (at 2/3,1/3, 1/4) were used. Correction for secondary isotropic extinction was applied according to Larson's formalism (1970), as implemented in the SHELXL-97 package (Sheldrick 1997), using a fixed weighting scheme $[1/\sigma(F_o)^2]$. Convergence was rapidly achieved after the first cycles of refinement and the variance-covariance matrix did not show any strong correlation between the refined parameters (scale factor, atomic positions of the framework atoms, and their isotropic displacement parameters). The structural refinement conducted with only the framework sites produced two intense residual peaks in the final difference-Fourier map of the nuclear density: one positive (~ +2.9 fm/Å^3) at 0,0,1/4 (the 2*a* position) and one negative (~ –0.6 fm/Å^3) at 0.03, –0.07, 0.33 (Fig. 2). Therefore a further refinement was performed assigning the oxygen scattering length to the 2*a* site and hydrogen scattering length to the site with the negative residual peak. As shown in Figure 3, the topological configuration of water molecules appears to be very complex: for every oxygen site (at 2*a*), the hydrogen atoms are distributed in 6×2 equivalent positions, above and below

Table 2. Details of neutron data collection and refinement

Crystal size (mm^3)	$1.1 \times 1.3 \times 2.0$
Cell parameters	$a = 9.2099(35)$ Å
	$c = 9.1894(18)$ Å
	$V = 675.04(39)$ Å^3
Z	2
Space group	*P6/mcc*
T (K)	293
Radiation (Å)	1.24126
Neutron flux density (n·s^{-1}·cm^{-2})	~2.5·10^6
Scan type, steps and width:	
$2\theta < 35°$	41 steps, pure ω-scan
$35 < 2\theta < 65°$	61 steps, pure ω-scan
$65 < 2\theta < 75°$	51 steps, pure ω-scan
$75 < 2\theta < 100.78°$	51 steps, ω-2θ scan
Time per step (s)	10
u, *v*, *w*	3.7, –6.4, 10.8
Max. 2θ (°) and sinθ/λ	100.78, 0.6206
	$-8 \le h \le 9$
	$-9 \le k \le 8$
	$-9 \le l \le 9$
No. measured reflections	1534
No. unique reflections	191
No. unique refl. with $F_o > 4\sigma(F_o)$	160
No. refined parameters	34
Extinction correction factor	0.0347
R_{int}	0.074
R_1 (F) with $F_o > 4\sigma(F_o)$	0.037
wR_2 (F^2)	0.098
GooF	1.083

Notes: $R_{int} = \Sigma \mid F_{obs}^2 - F_{obs}^2(\text{mean}) \mid / \Sigma [F_{obs}^2]$; $R_1 = \Sigma(||F_{obs}| - |F_{calc}||)/\Sigma|F_{obs}|$; $wR_2 = [\Sigma[w(F^2_{obs} - F^2_{calc})^2]/\Sigma[w(F^2_{obs})^2]]^{0.5}$, $w = 0.067$.
ω-scan width = $(u + v^*\tan\theta + w^*\tan^2\theta)^{0.5}$.

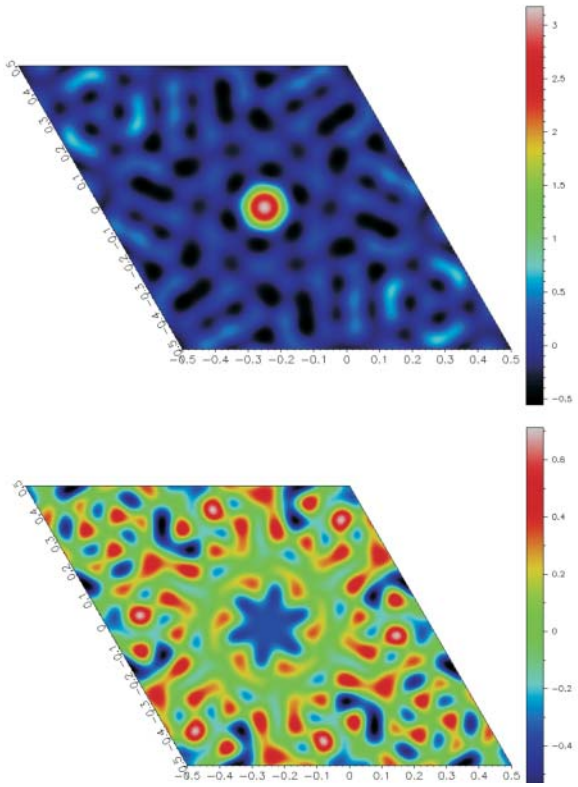

Figure 2. Difference-Fourier maps of the nuclear density of beryl at $z = 0.25$ (above) and $z = 0.332$ (below) after the first cycles of isotropic refinement with a channel-free structure. At $z = 0.25$ a residual peak of about +2.9 fm/Å^3 is seen lying on the sixfold axis, whereas at $z = 0.332$ there are six negative residual peaks (with a star shaped distribution) of about –0.6 fm/Å^3 around the sixfold axes. Note that the color scale is different for the two maps.

the oxygen site. As a consequence, in the structural refinement the occupancy factor of the proton site was fixed as a function of the water oxygen occupancy, taking into account the different site multiplicity. The final least-squares cycles were conducted with anisotropic thermal parameters, but isotropic displacement parameters were used for the partially occupied H_2O oxygen and proton sites (Table 3). All the principal mean square atomic displacement parameters were positively defined. At the end of the last refinement, no peak larger than ±0.3 fm/Å^3, located close to the framework sites, was present in the final difference-Fourier map of the nuclear density. No statistically significant peak was found in the Fourier map at the 2*b* site. Therefore Na is probably located, with the H_2O oxygen, at the 2*a* site. Due to the low amount of Na, all attempts at refining the Na-fraction at the 2*a* site were unsuccessful, giving no statistically significant results.

The final agreement index (R_1) was 0.037 for 34 refined parameters and 160 unique reflections with $F_o > 4\sigma(F_o)$ (Table 2). A table (Table 4) with observed and calculated structure factors was deposited and can be obtained from the authors upon request or through the Editorial Office.[1] Positional and displacement parameters are reported in Table 3. Relevant bond lengths and geometrical parameters are listed in Table 5.

Infrared spectra

Polarized IR spectra were obtained over the region 4000–2000 cm^{-1}, the range where absorption due to OH dipole vibration is expected. Spectra were obtained using radiation polarized parallel to the crystallographic **a** (**E**//**a**) and **c** (**E**//**c**) axes of the beryl sample (Fig. 4). **E**//**c** polarized spectra show two sharp absorption bands at 3700 and 3596 cm^{-1}. In contrast, **E**//**a** polarized spectra show low absorbance over the region between 4000 and 3500 cm^{-1}, but contain a prominent absorption band at 2359 cm^{-1}. According to Wood and Nassau (1967, 1968), we can assign the bands at 3700 and 3596 cm^{-1} to υ3 (symmetric stretching) and υ1 (asymmetric stretching) vibrational modes of H_2O respectively, whereas the absorption band at 2359 cm^{-1} is assigned to the anti-symmetric stretching frequency (υ3) of CO_2. These vibrational modes are in good agreement with those detected in previous studies of alkali-poor beryls (Wood and Nassau 1967, 1968; Artioli et al. 1993; Kolesov and Geiger 2000a). The strong anisotropic nature of the υ3 (H_2O) mode, which has a ~95% component of vibration parallel to **c**, suggests that the H···H direction is parallel (or quasi-parallel) to [001]. In contrast, the anisotropic nature of the υ3 (CO_2) absorption band suggests that the interchannel CO_2 molecules lie approximately in a plane parallel to (001).

Discussion and conclusions

The high-quality neutron diffraction data allowed us to refine the structure of this alkali/water-poor beryl, giving new insight into the topological configuration of the extra-framework content. First of all, the framework site positions are in excellent agreement with those reported by Artioli et al. (1993) for an alkali-poor beryl, with differences of less than 2σ. The analysis of the nuclear density Fourier map suggests that the water oxygen is located along the sixfold axis at the 2*a* site, with the proton at –0.028(7), –0.071(3), and 0.332(1) (Fig. 2, Table 3). The thermal displacement parameters of H_2O oxygen and hydrogen show reasonable values. As shown in Figure 2 and Table 3, the protons are statistically distributed in six equivalent positions. The geometrical configuration of the water molecule is well defined: the O-H bond distance is 0.949(18) Å and the H-O-H bond angle is 106.9(2.2)° (Table 5). The H···H vector is oriented at ~4° from [001] (Table 5). The shortest distance between water oxygen and framework O atoms is ~3.45 and ~2.35 Å between proton site and framework O atoms. Therefore, no direct interaction (e.g., hydrogen bonding) between water molecules and framework can be inferred. The amount of water obtained by structural refinement is 0.34(3) m.f.u., whereas the amount obtained by thermal analysis is ~0.26 m.f.u. We cannot exclude that this slight difference could be due to an incomplete dehydration during the thermogravimetric measurement. In fact, Wood and Nassau (1968) noted that even after heating to 1200

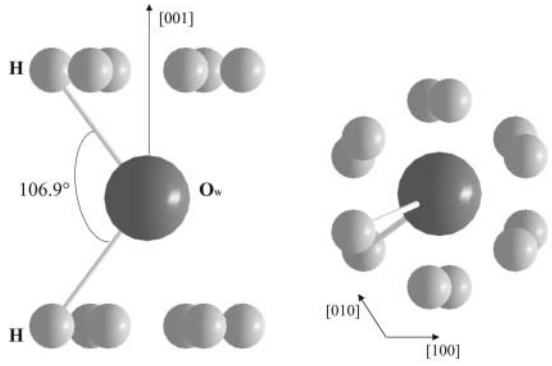

Figure 3. Topological configuration of water molecules into the channel of the alkali-poor beryl, viewed down [100] (left) and down [001] (right)

[1] Deposit item AM-06-003, Table 4. Deposit items are available two ways: For a paper copy contact the Business Office of the Mineralogical Society of America (see inside front cover of recent issue) for price information. For an electronic copy visit the MSA web site at http://www.minsocam.org, go to the American Mineralogist Contents, find the table of contents for the specific volume/issue wanted, and then click on the deposit link there.

Table 3. Refined positional and displacement parameters (Å^2) of the alkali-poor beryl sample

Site	*x*	*y*	*z*	Site occupancy	U_{11}	U_{22}	U_{33}	U_{23}	U_{13}	U_{12}	U_{eq}/U_{iso}
Si (12*l*)	0.3870(2)	0.1157(2)	0	1.0	0.0035(9)	0.0029(9)	0.0042(12)	0	0	0.0023(9)	0.0032(4)
Be (6*f*)	1/2	0	1/4	1.0	0.0065(6)	0.0039(7)	0.0059(6)	0	0	0.0019(4)	0.0057(3)
Al (4*c*)	2/3	1/3	1/4	1.0	0.0018(13)	0.0018(13	0.0052(17)	0	0	0.0009(6)	0.0029(8)
O1 (12*l*)	0.3096(2)	0.2361(2)	0	1.0	0.0075(8)	0.0074(7)	0.0119(8)	0	0	0.0059(6)	0.0079(3)
O2 (24*m*)	0.4987(1)	0.1454(1)	0.1452(1)	1.0	0.0064(5)	0.0046(6)	0.0056(6)	–0.0016(3)	–0.0031(3)	0.0027(4)	0.0056(3)
Ow (2*a*)	0	0	1/4	0.34(3)							0.071(9)
H (24*m*)	–0.0287(77)	–0.0709(30)	0.3327(16)	0.056(5)							0.04(1)

Note: The anisotropic displacement factor exponent takes the form: $-2\pi^2[(ha^*)^2U_{11} + \ldots + 2hka^*b^*U_{12}]$. U_{eq} is defined as one-third of the trace of the orthogonalized U_{ij} tensor.

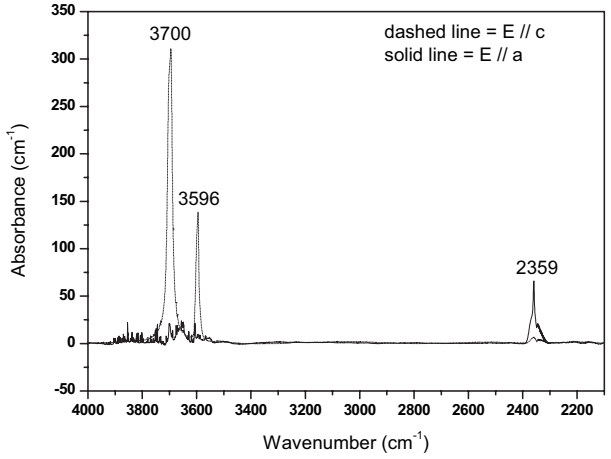

FIGURE 4. Polarized single-crystal IR spectra of alkali-poor beryl in the region between 4000–2100 cm^{-1}, parallel (dashed line) and perpendicular (solid line) to [001]. Slight interference over the region 4000–3600 cm^{-1}, and a slight double hump in the **E**//**a** spectra around 2350 cm^{-1} are due to the presence of trace amounts of water vapor and CO_2 in the optics of the microscope during the measurement.

TABLE 5. Relevant bond distances and angles

Si-O1	1.5899(23) Å	O_w-H (× 12)	0.949(18) Å
Si-O1	1.5958(21) Å	H-O-H	106.9(2.2)°
Si-O2 (×2)	1.6225(14) Å	(H···H)∠ [001]	~4°
Be-O2 (×4)	1.6545(12) Å		
Al-O2 (×6)	1.9072(11) Å		

°C, spectroscopic investigation of beryls from their experiments still showed evidence for the presence of water, and heating to 1350 °C was necessary to completely remove all H_2O and CO_2. However, the occupancy factor of the H_2O oxygen obtained by structural refinement should be considered as the sum of O_w + Na, with Na probably also located at the 2*a*. Therefore, chemical (0.26 H_2O m.f.u. + 0.03 Na a.f.u, Table 1) and diffraction [0.34(3) H_2O m.f.u.] values appear to be in good agreement.

The topological configuration of the H_2O molecule into the channel is confirmed by the spectroscopic investigation. Polarized single-crystal IR spectra show that the H_2O molecule is oriented with the molecular symmetry axis perpendicular to the hexagonal axis and H···H vector parallel (or quasi-parallel) to [001]. This result agrees with the structural refinement and with the previous results of Wood and Nassau (1968) and Kolesov and Geiger (2000a) on the orientation and vibrational states of H_2O in natural or synthetic alkali-poor/alkali-free beryl. In addition, the IR spectra show that no hydrogen bonding occurs among water molecules and framework O atoms. We can infer, therefore, that the orientation of the H_2O molecule is due to more remote electrostatic charge distribution. The orientation of the water molecule also agrees to the ab initio Hartree-Fock study and charge density analysis of beryl by Prencipe (2002), who provided a calculated possible orientation of the H_2O dipole moment into the channel. Two calculated orientations were given: one with the H···H axis oriented at an angle of about 40° from [001] and the other with the H···H vector parallel to [001].

We also report evidence for the presence of small amounts (probably up to only a few tens of parts per million by weight) of CO_2 molecules in the beryl channels. CO_2 molecules are commonly found as extra-framework (interchannel) molecules in cordierite, which has structural channels very similar to those found in beryl (Armbruster 1985, 1986; Armbruster and Bloss 1982). However, reports of interchannel CO_2 in beryl are much less common. In addition, IR spectra show that the orientation of the CO_2 molecule in our beryl sample is different from that of H_2O: the O···O vector lies on a plane perpendicular to [001], according to Wood and Nassau (1968). This is the same orientation that CO_2 groups have when present in structural channels in cordierite (Kolesov and Geiger 2000b).

Comparing our data with chemical, spectroscopic and structural data already published, we can infer that: (1) The rigid framework of the beryl crystal structure and its substitution pattern, obtained by X-ray and neutron experiments ($Al^{3+} \leftrightarrow Mg^{2+}$, $Fe^{2+/3+}$, Mn^{2+}, Cr^{3+}, V^{3+}, and $Be^{2+} \leftrightarrow Li^{+}$, Aurisicchio et al. 1988; Artioli et al. 1993), is confirmed. There are no evident distortions or modification of the Si/Al/Be-polyhedra as a function of the extra-framework content. (2) Water/alkali-rich beryls ($H_2O + Na_2O + Cs_2O > 3$ wt%) show a topological configuration of the extra-framework content with H_2O oxygen at the 2*a* site and protons distributed around the sixfold axis; the H···H axis is considered to be lying on a plane parallel to (001) (Artioli et al. 1993). Cs also occupies the 2*a* site, whereas Na occupies the 2*b* site. (3) Water/alkali-poor beryls ($H_2O + Na_2O + Cs_2O < 1.5$ wt%) show a topological configuration of the channel content with the H_2O oxygen at the 2*a* site and protons distributed in six equivalent positions around the sixfold axis and, as shown in this study, the H···H vector is oriented at ~4° from [001] (i.e., an opposite configuration with respect to that found for alkali-rich beryl). Na occupies the 2*a* site and the 2*b* site is empty.

ACKNOWLEDGMENTS

The authors are indebted to M. Petrelli and G. Poli (Earth Science Department, Perugia) and R. Vivani (Department of Chemistry, Perugia) for the LA-ICP-MS and thermogravimetric analysis. G.R. Rossman and L.A. Groat are thanked for their useful suggestions. F. Nestola thanks the A. von Humboldt Foundation.

REFERENCES CITED

Aines, R.D. and Rossman, G.R. (1984) The high-temperature behaviour of water and carbon dioxide in cordierite and beryl. American Mineralogist, 69, 319–327.

Angel, R.J., Downs, R.T., and Finger, L.W. (2000) High-temperature high-pressure diffractometry. In R.M. Hazen and R.T. Downs, Eds., High-Temperature and High-Pressure Crystal Chemistry, 41, 559–596. Reviews in Mineralogy and Geochemistry, Mineralogical Society of America, Chantilly, Virginia.

Armbruster, T. (1985) Ar, N_2, and CO_2 in the structural cavities of cordierite, an optical and X-ray single-crystal study. Physics and Chemistry of Minerals, 12, 233–245.

——— (1986) Role of Na in the structure of low-cordierite: A single-crystal X-ray study. American Mineralogist, 71, 746–757.

Armbruster, T. and Bloss, F.D. (1982) Orientation and effects of channel H_2O and CO_2 in cordierite. American Mineralogist, 67, 284–291.

Artioli, G., Rinaldi, R., Ståhl, K., and Zanazzi, P.F. (1993) Structure refinements of beryl by single-crystal neutron and X-ray diffraction. American Mineralogist, 78, 762–768.

Aurisicchio, C., Fioravanti, G., Grubessi, O., and Zanazzi, P.F. (1988) Reappraisal of the crystal chemistry of beryl. American Mineralogist, 73, 826–837.

Bragg, W.L. and West, J. (1926) The structure of beryl. Proceedings of the Royal Society London, 3A, 691–714.

Brown, G.E., Jr. and Mills, B.A. (1986) High-temperature structure and crystal chemistry of hydrous alkali-rich beryl from the Harding pegmatite, Taos Country, New Mexico. American Mineralogist, 71, 547–556.

Charoy, B., de Donato, P., Barres, O., and Pinto-Coelho, C. (1996) Channel occupancy in alkali-poor beryl from Serra Branca (Goias, Brasil): Spectroscopic

characterization. American Mineralogist, 81, 395–403.
De Almeida Sampaio Filho, H., Sighinolfi, G., and Galli, E. (1973) Contribution to crystal chemistry of beryl. Contribution to Mineralogy and Petrology, 38, 279–290.
Ferraris, G., Prencipe, M., and Rossi, P. (1998) Stoppaniite, a new member of the beryl group: Crystal structure and crystal-chemical implication. European Journal of Mineralogy, 10, 491–496.
Gibbs, G.V., Breck, D.W., and Meagher, E.P. (1968) structural refinement of hydrous and anhydrous beryl, $Al_2(Be_3Si_6)O_{18}$ and emerald, $Al_{1.9}Cr_{0.1}(Be_3Si_6)O_{18}$. Lithos, 1, 275–285.
Goldman, D.S., Rossman, G.R., and Parkin, K.M. (1978) Channel constituents in beryl. Physics and Chemistry of Minerals, 3, 225–235.
Hawthorne, F.C. and Černý, P. (1977) The alkali-metal positions in Cs-Li beryl. Canadian Mineralogist, 15, 414–421.
Hazen, R.M., Au, A.Y., and Finger, L.W. (1986) High-pressure crystal chemistry of beryl ($Be_3Al_2Si_8O_{18}$) and euclase ($BeAlSiO_4OH$). American Mineralogist, 71, 977–984.
King, H.E. and Finger, L.W. (1979) Diffracted beam crystal centering and its application to high-pressure crystallography. Journal of Applied Crystallography, 12, 374–378.
Kolesov, B.A. and Geiger, C.A. (2000a) The orientation and vibrational states of H_2O in synthetic alkali-free beryl. Physics and Chemistry of Minerals, 27, 557–564.
——— (2000b) Cordierite II: The role of CO_2 and H_2O. American Mineralogist, 85, 1265–1274.
Larson, A.C. (1970) Secondary-extinction corrections. In F.R. Ahmed, S.R. Hall, and C.P. Huber, Eds., Crystallographic Computing, p. 291 – 294. Munksgaard Publisher, Copenhagen, Denmark.
Longerich, H.P., Jackson, S.E., and Günther, D. (1996) Laser ablation inductively coupled plasma mass spectrometric transient signal data acquisition and analyte concentration calculation. Journal of Analytical Atomic Spectroscopy, 11, 899–904.
Morosin, B. (1972) Structure and thermal expansion of beryl. Acta Crystallographica, 28, 1899–1903.
Prencipe, M. (2002) Ab initio Hartree-Fock study and charge density analysis of beryl ($Al_4Be_6Si_{12}O_{36}$). Physics and Chemistry of Minerals, 29, 552–561.
Schmetzer, K. (1989) Types of water in natural and synthetic emerald. Neues Jahrbuch für Mineralogie Monatshefte, 1989, 541–551.
Sheldrick, G.M. (1997) SHELX-97. Programs for crystal structure determination and refinement. Univeristy of Goettingen, Germany.
Sheriff, B.L., Grundy, D.H., Hartman, J.S., Hawthorne, F.C., and Černý, P. (1991) the incorporation of alkalis in beryl: Multi-nuclear MAS NMR and crystal structure study. Canadian Mineralogist, 29, 271–285.
Wilson, A.J.C. and Price, E., Eds. (1999) International Tables for Crystallography Volume C. Kluwer Academic Publishers, Dordrecht, The Netherlands.
Wood, D.L. and Nassau, K. (1967) Infrared spectra of foreign molecules in beryl. Journal of Chemical Physics, 42, 2220–2228.
——— (1968) The characterization of beryl and emerald by visible and infrared absorption spectroscopy. American Mineralogist, 53, 777–800.

MANUSCRIPT RECEIVED JANUARY 13, 2005
MANUSCRIPT ACCEPTED MAY 3, 2005
MANUSCRIPT HANDLED BY LEE GROAT